

## VISCO-ELASTIC ANALYSIS OF THE FEMUR-IMPLANT SYSTEM BY USING FINITE ELEMENT APPROACH

S. P I S Z C Z A T O W S K I <sup>(1)</sup>, K. S K A L S K I <sup>(2)</sup>

<sup>(1)</sup> BIAŁYSTOK UNIVERSITY OF TECHNOLOGY,  
FACULTY OF MECHANICAL ENGINEERING,  
ul. Wiejska 45c, 15–351 Białystok, Poland

<sup>(2)</sup> WARSAW UNIVERSITY OF TECHNOLOGY,  
FACULTY OF PRODUCTION ENGINEERING,  
INSTITUTE MECHANICS AND DESIGN,  
ul. Narbutta 85, 02–524 Warszawa, Poland

The subject of this work is to elucidate the significance of rheological processes taking place in a bone-implant system when the implanted joint is bearing a load. The processes of mathematical modelling (by variational formulation and finite element approach) and computer - aided strength analysis of a human hip joint endoprosthesis-femoral bone system, taking into account the rheological properties of bone tissue, are presented. The three distinct types of material that are present in the system (cortical bone, trabecular bone and implant) exhibit significant differences in their elastic and rheological properties. The analysis is carried out using the finite element method. Consideration of the rheological properties of bone tissue during the analysis makes it possible to observe, under conditions of fixed loads, the changes in the fields of stresses, strains and strain energy density in the bone – implant system.

**Key words:** rheology, bone tissue, endoprosthesis, stress, strain.

### 1. INTRODUCTION

Alloplasty currently plays an important role in the treatment of various kinds of joint injuries and degeneration. Alloplasty of the hip joint is of particular significance in this field. This joint performs a key function in the human skeletal system, ensuring an adequate range of movement of the lower limbs as well as

providing support for the upper body. Damage to the joint may cause permanent lameness or even, in some cases, death. Alloplasty is often the only method of treating a damaged joint. Despite continued improvement in the construction of endoprostheses, their period of correct functioning remains too short, up to the current maximum of less than twenty years. Among the main causes of this are the following engineering problems: inappropriate stiffness of the prosthesis stem, insufficient bond of the implant to the bone, premature wearing out of friction pairs (prosthesis head-acetabulum).

It is generally acknowledged that a significant increase in the longevity of artificial joints can be achieved through optimal correspondence of the stiffness of the prosthesis stem and that of the bone into which it is to be fixed. Yet, it is necessary to recognise that this optimal stiffness is not to be understood as a simple correspondence between the mechanical parameters of the prosthesis stem and those of bone tissue. An essential problem is that the mechanical properties of bone tissue are not static. They undergo continual changes related to at least three factors: changes in the age of the patient, functional adaptation of the bone tissue and rheological processes taking place in the bone. KEAVENY and HAYES [4] set forth the data from which it results that the modulus of elasticity for trabecular bone decreases from age 20 at a rate of about 17% per decade. NATALI and MEROI [7] obtained the results indicating that changes in the Young modulus for human cortical bone after age 20 reach about 20 – 25%. The process of functional adaptation of bone tissue is related to its structural adaptation to changing conditions of load. In accordance with Wolff's law, tissue not subjected to load atrophies, and conversely, bone under excessive load tend to increase their density and geometric dimensions. This problem has been the subject of many investigations in recent years. RIETBERGEN *et al.* [9] have shown that as a result of implantation of an endoprosthesis into a joint, after two years (in experiments on animals), changes in the cross-sectional area of cortical bone reached 20 – 23%.

The above changes in the mechanical and geometrical properties of bone occur over a long period of time. Adaptational processes appear after several months, and changes related to age continue for decades. Decidedly shorter is the period of change in the mechanical properties of bone tissue related to rheological processes taking place within the bone. DELIGIANNI *et al.* [1] have presented the rheological characteristics of trabecular bone. He asserts that the process of relaxation of stress diminishes in this type of tissue over the course of one hour, but up to 95% of the fall in stress occurs within the first 100 seconds. The average change in mechanical parameters obtained on the basis of relaxation experiments reached, in the tests referred to, 20 – 25%. SASAKI and ENYO [10], LAKES *et al.* [6] as well as KNETS [5] have investigated the rheological properties of cortical bone. All these studies have demonstrated a change in the mechanical

properties of this type of tissue of a similar range to that of trabecular bone (approx. 20%), but these changes take place in times of the order of some scores of hours.

It follows from the above-cited data, the range of change in the mechanical properties of bone tissue occurring as a result of rheological processes is comparable to the changes due to ageing of the bone, and to the functional adaptation of bone tissue, but these rheological processes occur significantly faster, and are cyclically repeated. It is necessary, therefore, to take them into account when analysing the strength of the bone-implant system.

Until now, researchers have neglected the rheological processes occurring in the bone – implant system. This paper presents an attempt to analyse the influence of the viscoelasticity of bone tissue on functioning of the implanted hip joint.

## 2. METHODS

The basic techniques applied in the research presented here is that of computer simulation using the finite element method (FEM). This method makes it possible to effectively determine the fields of displacements, strains and stresses resulting from a load acting on the system under study. The foundation of the analysis is however, the elaboration of an appropriate physical and mathematical model.

### *2.1. Physical model of the femur – hip joint endoprosthesis system*

Among the most important elements in the physical modelling of the bone – implant system are:

- construction of a geometrical model of the femur and endoprosthesis,
- description of the mechanical properties of the particular materials present in the system (cortical bone, trabecular bone, implant),
- modelling of boundary conditions (loads and constraints of the system, the connection between the endoprosthesis and the bone surrounding it).

A three-dimensional geometrical model of the femur has been obtained based on the Standardised Femur (VICECONTI *et al.* [11]). The stem shape was taken from OSTEONICS Omnifit implant (size No. 8). FEM model (Fig. 1) has been build up in ANSYS by applying 20-nodal VISCO 89 elements.

The elaborated material model takes into account the heterogeneity of bone tissue. It is important to note that both bone tissue types (cortical and trabecular) exhibit anisotropy of their mechanical properties (NATALI and MEROI [7],

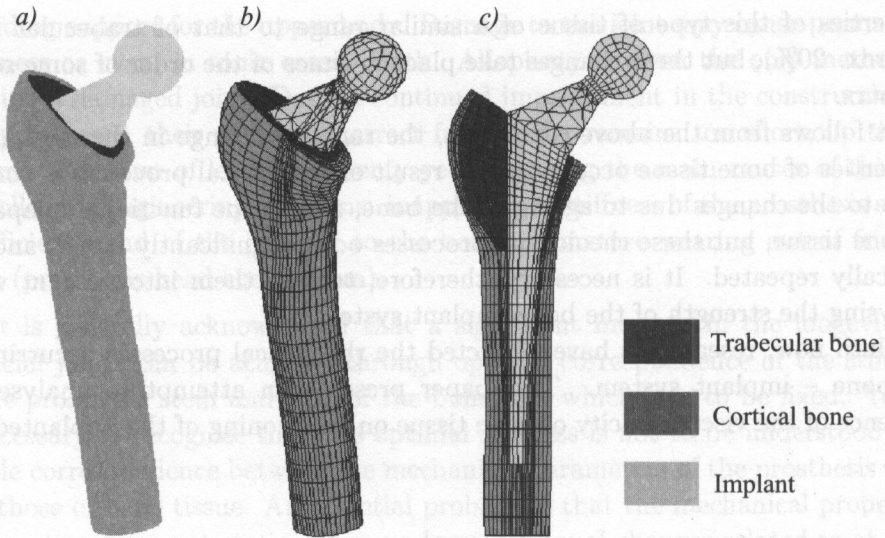


FIG. 1. Geometrical model of the femur – hip joint endoprosthesis system: solid model; b) and c) FEM model.

KEAVENY and HAYES [4]). Most often the Young modulus is more or less twice as high in one direction as it is in the two others. Taking into consideration, however, the obvious difficulties concerning the anisotropy measurement of the rheological properties of bone tissue, the authors were forced to accept a simplified model based on isotropy of the material. The elastic parameters of the bone tissue were taken from the literature (NATALI and MEROI [7], KEAVENY and HAYES [4]), at the following levels: cortical bone  $E = 17$  GPa,  $\nu = 0.36$ ; trabecular bone  $E = 1$  GPa,  $\nu = 0.4$ .

From the studies of LAKES *et al.* [6], SASAKI and ENYO [10] or DELIGIANNI *et al.* [1] it can be stated that bone tissue displays nonlinear viscoelasticity. Yet, for certain ranges of load, it is acceptable to employ a simplified model using linear viscoelasticity for both cortical and trabecular tissue. Such a model has been employed in the research presented here. In describing the time-variable properties of the material, Maxwell's generalised model equations have been applied:

$$(2.1) \quad G(\xi) = \sum_{i=1}^N G_i e^{(-\xi/\lambda_i)} + G(\infty)$$

where:  $G$  – material parameter (e.g. Young modulus, shear modulus or bulk modulus),  $G(\infty)$  – value of the parameter  $G$  in infinity,  $N$  – number of Maxwell's element used in approximation of material properties,  $G_i$  – initial value of parameter  $G$  for the  $i$ -th Maxwell's element,  $\lambda_i$  – relaxation time for the  $i$ -th Maxwell's element,  $\xi$  – running time of the process.

It is necessary to emphasise that there are significant differences in the viscoelastic properties of cortical and trabecular tissue. Rheological processes in trabecular bone take place in much shorter times (to 100 sec, DELIGIANNI *et al.* [1]) than they do in cortical bone (an equivalent range of change in times of  $10^5$  sec, LAKES *et al.* [6]). The rheological characteristics of bone tissue applied in the analysis are shown in Tables 1 and 2.

**Table 1. Changes through time of strength parameters for a viscoelastic model of cortical bone.**

time t [s]	0	1	10	100	1000	10000	40000	70000	100000	$\infty$
$G(t)$ [GPa]*	6.25	6.230	6.181	6.042	5.798	5.446	5.154	5.048	4.987	4.875
$K(t)$ [GPa]*	20.24	20.175	20.016	19.565	18.777	17.638	16.691	16.346	16.150	15.878
$G(t)/G(10)$	1.011	1.008	1	0.977	0.938	0.881	0.834	0.817	0.807	0.788
$K(t)/K(10)$	1.011	1.008	1	0.977	0.938	0.881	0.834	0.817	0.807	0.788

**Table 2. Changes through time of strength parameters for a viscoelastic model of trabecular bone**

time t [s]	0	1	2	3	4	5	6	8	10	40	100
$G(t)$ [MPa]*	357	336.5	324.6	316.9	311.3	307.1	303.7	300.9	294.8	278.0	260.9
$K(t)$ [GPa]*	1.667	1.571	1.516	1.480	1.454	1.434	1.418	1.405	1.376	1.298	1.218
$G(t)/G(0)$	1	0.942	0.909	0.887	0.872	0.860	0.851	0.843	0.826	0.779	0.731
$K(t)/K(0)$	1	0.942	0.909	0.887	0.872	0.860	0.851	0.843	0.826	0.779	0.731

\*  $G$  - shear modulus,  $K$  - bulk modulus

Pure elastic model of the implant has been employed ( $E = 1.1 \times 10^{11}$  Pa,  $\nu = 0.3$  - Ti6Al4V alloy or  $E = 2.0 \times 10^{11}$  Pa,  $\nu = 0.3$  - CoCrMo alloy).

The model of hip joint loads (Fig. 2) employed in this research takes into account the force acting on the endoprosthesis head ( $R = 1730$  N) as well as the resultant muscular forces acting on the major trochanter ( $M = 1270$  N). These values correspond to the load conditions on the hip joint of a patient of about 60 kg body mass.

A rigid constraint of the modelled femoral fragment was assumed (distal end). It was assumed that the prosthesis is fully bonded (continuity of displacements and normal stresses) with the bone along approximately 40% of the length of the stem (proximal side) and no contact appears between the remaining part of the stem and femur. Two ways of fixing the implant were considered. The first, in the area of bonding the prosthesis stem with the bone, only trabecular tissue surrounds the implant (Fig. 3a, model M1). In order to take into account the local point of direct contact between the prosthesis and cortical bone (such support

does sometimes occur in reality), in model M2 (Fig. 3b) the properties of the bone tissue adjoining the stem were changed in the lower region of the contact zone. Instead of the parameters of trabecular bone, suitable data for cortical bone were applied.

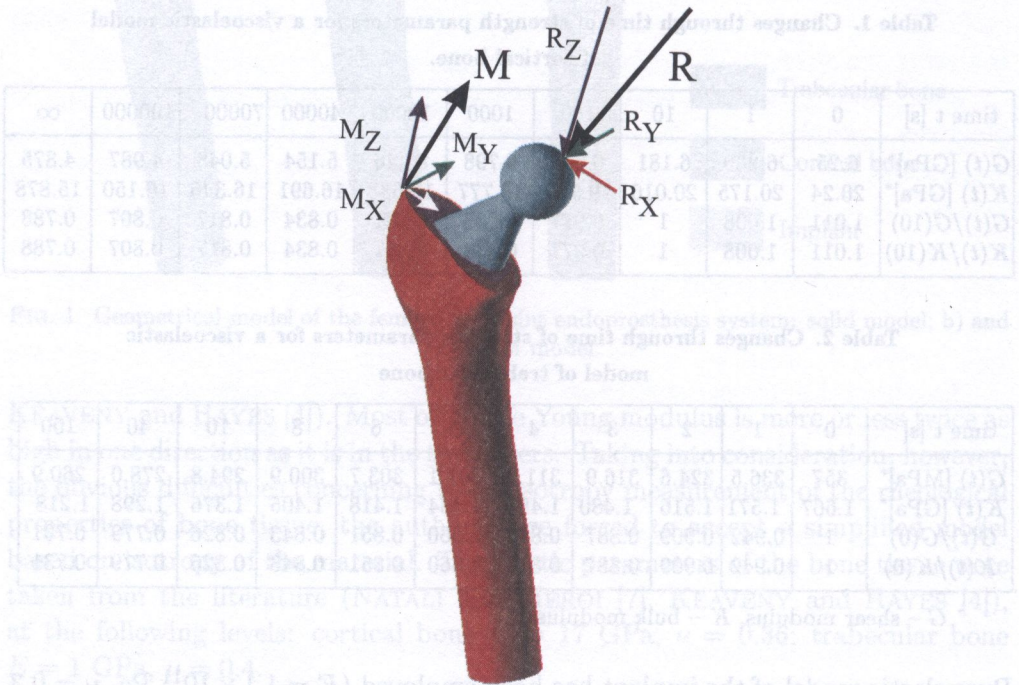


FIG. 2. Scheme of the loads acting on the femur - endoprosthesis system.

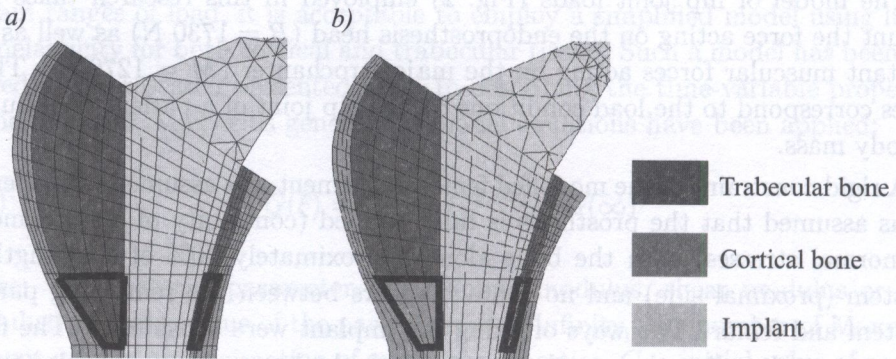


FIG. 3. Support of the endoprosthesis stem by: a) trabecular bone only - model M1, b) partly, by the cortical and trabecular bone - model M2.

2.2. Mathematical model of the femur – endoprosthesis system with regard to the viscoelastic properties of bone tissue

In such a model (PISZCZATOWSKI *et al.* [8]) one uses the viscoelastic modelling of the bone material properties. The implant is treated as a pure elastic material. Let us denote (Fig. 4):

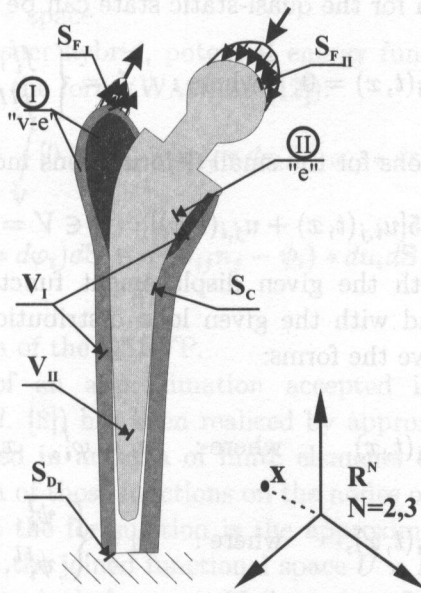


FIG. 4. Scheme of the hip joint endoprosthesis – femoral bone system: 1)  $V_I, V_{II}$  – domains of bone I and implant II respectively; I – viscoelastic, II – elastic; 2)  $S_I, S_{II}$  – boundaries of the domains  $V_I$  and  $V_{II}$ ; 3)  $S_C$  – curve (surface) dividing the domains  $V_I$  and  $V_{II}$ ; 4)  $S_{D_I}, S_{F_I}, S_{F_{II}}$  – boundaries subsets of the domains  $V_I$  and  $V_{II}$  on which the boundary displacement (D) and stress (F) conditions are defined.

The problem consists in determining following functions: displacements  $u^I(t, x)$  and  $u^{II}(t, x)$ , strains  $\epsilon^I(t, x)$  and  $\epsilon^{II}(t, x)$ , stresses  $\sigma^I(t, x)$  and  $\sigma^{II}(t, x)$  satisfying the given boundary conditions on  $S_{D_I}$  and  $S_{F_I}, S_{F_{II}}$ .

The constitutive equation of viscoelastic and elastic material has the following form:

$$(2.2) \quad \sigma_{ij}(t, x) = \int_{-\infty}^t \tilde{G}_{ijkl}(t - \tau, x) \frac{\partial}{\partial \tau} \epsilon_{kl}(\tau, x) d\tau, \quad x \in V.$$

where the generalized tensor of material is elastic and viscoelastic properties are defined below:

$$(2.2a) \quad \tilde{G}_{ijkl}(x, t) = \begin{cases} 0, & t \leq 0 \\ D_{ijkl}(x), & t > 0, \quad x \in V_{II} \\ G_{ijkl}(t, x), & t > 0, \quad x \in V_I \end{cases}$$

The equilibrium equation for the quasi-static state can be expressed by:

$$(2.3) \quad \sigma_{ij,j}(t, x) + f_i(t, x) = 0, \quad \text{where:} \quad f_i = \begin{cases} f_i^I, & x \in V_I \\ f_i^{II}, & x \in V_{II} \end{cases}$$

The compatibility equations for the small deformations model are as follows:

$$(2.4) \quad \varepsilon_{ij}(t, x) = 0.5[u_{i,j}(t, x) + u_{j,i}(t, x)], \quad x \in V = V_I \cup V_{II}.$$

Boundary conditions with the given displacement function  $\varphi_i$  (displacement boundary conditions) and with the given load distribution function  $\psi_i$  (stress boundary conditions) have the forms:

$$(2.5) \quad u_i(t, x) = \varphi_i(t, x), \quad \text{where:} \quad \varphi_i = \varphi_i^I, \quad x \in S_{D_I},$$

$$(2.6) \quad \sigma_{ij}n_j(t, x) = \psi_i(t, x), \quad \text{where:} \quad \psi_i = \begin{cases} \psi_i^I, & x \in S_{F_I} \\ \psi_i^{II}, & x \in S_{F_{II}} \end{cases},$$

$n_j$ -being the  $j$ -th component of the external normal unit vector.

Finally, reaction conditions occurring between the domains  $V_I$  and  $V_{II}$  on the surface  $S_C$  have the form:

$$(2.7) \quad u_i^I(t, x) = u_i^{II}(t, x), \quad \text{for} \quad x \in S_C$$

$$(2.8) \quad \sigma_{ij}^I n_i^I n_j^I(t, x) = \sigma_{ij}^{II} n_i^{II} n_j^{II}(t, x), \quad \text{for} \quad x \in S_C.$$

Actually, the presented problem by the system of Eqs. (2.2) – (2.8) cannot be analytically solved. However, some of general approaches for quasi-static viscoelasticity are known (see GIORGI and MARZOCCHI [3], FABRIZIO [2]).

### 2.3. Variational functional for quasi-static boundary value problems and approximation of variational equation by using finite element method

The defined quasi-static boundary value problems (QSBVP) can be effectively solved by using the variational formulations and next the FEM approximation.

The formulated variational functional is treated jointly for viscoelastic and elastic bodies. For the sake of simplicity let us introduce the following additional notation:

$$(2.9) \quad \begin{aligned} S_D &= S_{D_I} \cup S_{D_{II}}, & S_F &= S_{F_I} \cup S_{F_{II}}, & V &= V_I \cup V_{II} \\ \mathbf{V} &= V \times R_+, & \mathbf{S}_D &= S_D \times R_+, & \mathbf{S}_F &= S_F \times R_+, & \mathbf{S} &= S \times R_+, \end{aligned}$$

where  $R_+$  – real time – space.

The Washizu-Reissner hybrid, potential energy functional  $\mathbf{J}_V$  with the Lagrange multipliers has the form (WASHIZU [12]):

$$(2.10) \quad \begin{aligned} \mathbf{J}_V(u, \varepsilon, \sigma) &= \int_V [0.5 \tilde{G}_{ijkl} * d\varepsilon_{ij} * d\varepsilon_{kl} - \sigma_{ij} * d\varepsilon_{ij} - (\sigma_{ij,j} + f_i) * du_i] dV \\ &+ \int_{S_D} (\sigma_{ij} n_j * d\varphi_i) dS + \int_{S_F} (\sigma_{ij} n_j - \psi_i) * du_i dS, \quad \forall [u, \varepsilon, \sigma \in U \times E \times S] \end{aligned}$$

and yields the solution of the QSBVP.

The main idea of an approximation accepted in the presented paper (PISZCZATOWSKI *et al.* [8]) has been realized by approximation of the  $\mathbf{V}$  space by the functions placed in an area of finite elements dividing this space, and next by approximation of those functions on the nodes of elements. A significant complicating factor in the formulation is the approximation of the three fields  $u, \varepsilon, \sigma$  by  $u_h, \varepsilon_h, \sigma_h$  in the joined functional space  $U \times E \times S$ . It is necessary to note that approximation includes space  $\mathbf{V}$  (boundary  $\mathbf{S}$ ) in  $R^N$  as well as time  $t$  in space  $R_+$ .

Let us consider  $E_h(\mathbf{V})$  as a finite element of space  $\mathbf{V}$  and  $W_h$  as an approximation of the space  $W_2^1(\mathbf{V}, W_2^1(R_+))$ . Joined functional space of displacement ( $1 \times N$ ), strain ( $N \times N$ ), stress ( $N \times N$ ) fields are approximated by:

$$\mathbf{W}_h := \{ [W_h]^N \times [W_h]^{N \times N} \times [W_h]^{N \times N} \}.$$

Let us introduce  $\gamma_p(x)$  – approximating polynomial on space variables  $x = (x_1, x_2, x_3)$  and  $\alpha_q(t)$  – approximating polynomial on time variable. Approximate fields  $u_i, \varepsilon_{ij}, \sigma_{ij}$  of the functional (2.9) can be written as follows:

$$(2.11) \quad \begin{aligned} u_i(x, t) &= \sum_{(p,q) \in Q_h} \underline{u}_{ipq} \gamma_p(x) \alpha_q(t), \\ \varepsilon_{ij}(x, t) &= \sum_{(p,q) \in Q_h} \underline{\varepsilon}_{ijpq} \gamma_p(x) \alpha_q(t), \\ \sigma_{ij}(x, t) &= \sum_{(p,q) \in Q_h} \underline{\sigma}_{ijpq} \gamma_p(x) \alpha_q(t), \end{aligned}$$

where:  $\underline{u}$ ,  $\underline{\varepsilon}$ ,  $\underline{\sigma}$  - expansion coefficients,  $p, q \in Q_h$  - set of the node coefficients of the meshed area and time coefficients in approximate space such as  $u_i(x = x_p, t = t_q) = \underline{u}_{ipq}$  (similarly for  $\varepsilon_{ij}$  and  $\sigma_{ij}$ ). Set  $Q_h$  is a Cartesian product, i.e.:  $Q_h = [1 \dots \sum E_h] \times [0 \dots N_h]$ , where  $p \in [1, \dots \sum E_h]$ ,  $q \in [0, \dots N_h]$  however  $\sum E_h$  - number of nodes digitized area and  $(N_h + 1)$  number of nodes of digitized time.

The introduced polynomials  $\gamma_p$  and  $\alpha_q$  define the basis of approximated functional spaces  $[W_h]^N$ ,  $[W_h]^{N \times N}$ , which could be written as follows:

$$(2.12) \quad \{\gamma_p \alpha_q e_i\}_{(p,q) \in Q_h, i \in \{1, \dots, N\}}, \quad \{\gamma_p \alpha_q e_i e_j^T\}_{(p,q) \in Q_h, i, j \in \{1, \dots, N\}},$$

where:  $e_i = (\delta_{i1}, \dots, \delta_{iN})^T$ ,  $\delta_{ik}$  - Kronecker symbol.

All we have to do now is to define the approximation of the given function and boundary condition in the considered variational functional (2.9), i.e.:

$$(2.13) \quad \begin{aligned} f_i(x, t) &= \sum_{(p,q) \in Q_h} \underline{f}_{ipq} \gamma_p(x) \alpha_q(t), \\ \psi_i(x, t) &= \sum_{(p,q) \in Q_h} \underline{\psi}_{ipq} \gamma_p(x) \alpha_q(t), \\ \varphi_i(x, t) &= \sum_{(p,q) \in Q_h} \underline{\varphi}_{ipq} \gamma_p(x) \alpha_q(t), \end{aligned}$$

When we substitute (2.11) and (2.13) to functional (2.10), we obtain their approximate form:

$$(2.14) \quad \begin{aligned} J(u_h, \varepsilon_h, \sigma_h) &= \sum_{(p,q) \in Q_h} \sum_{(r,s) \in Q_h} [0.5 \int_{\mathbf{V}} \tilde{G}_{ijkl} \underline{\varepsilon}_{klrs} \underline{\varepsilon}_{ijpq} \gamma_p \gamma_r * d\alpha_s * d\alpha_q d\mathbf{V} \\ &\quad - \int_{\mathbf{V}} \underline{f}_{irs} \underline{u}_{ipq} \gamma_r \gamma_p \alpha_s * d\alpha_q d\mathbf{V} - \int_{\mathbf{V}} \underline{\sigma}_{ijrs} \underline{\varepsilon}_{ijpq} \gamma_r \gamma_p \alpha_s * d\alpha_q d\mathbf{V} \\ &\quad + \int_{\mathbf{V}} \underline{\sigma}_{ijrs} \underline{u}_{ipq} \gamma_r \gamma_p \alpha_s * d\alpha_q d\mathbf{V} + \int_{\mathbf{S}_D} \underline{\sigma}_{ijrs} n_j (\underline{u}_{ipq} - \underline{\varphi}_{ipq}) \gamma_r \gamma_p \alpha_s * d\alpha_q d\mathbf{S} \\ &\quad - \int_{\mathbf{S}_F} \underline{\psi}_{irs} \underline{u}_{ipq} \gamma_r \gamma_p \alpha_s * d\alpha_q d\mathbf{S}. \end{aligned}$$

On the basis of the stationary condition  $\delta J = 0$  we can write the following, equivalent system of equations:

$$\begin{aligned}
 & 1. \sum_{(r,s) \in Q_h} \left[ \int_{\mathbf{V}} \gamma_{p,j} \gamma_r \alpha_s * d\alpha_q d\mathbf{V} - \int_{\mathbf{S}_D} n_j \gamma_p \gamma_r \alpha_s * d\alpha_q d\mathbf{S} \right] \underline{\sigma}_{ijrs} \\
 & \qquad = \sum_{(r,s) \in Q_h} \left[ \int_{\mathbf{V}} \underline{f}_{irs} \gamma_p \gamma_r \alpha_s * d\alpha_q d\mathbf{V} + \int_{\mathbf{S}_F} \underline{\psi}_{irs} \gamma_p \gamma_r \alpha_s * d\alpha_q d\mathbf{S} \right] \\
 & 2. \sum_{(r,s) \in Q_h} \left[ \int_{\mathbf{V}} \tilde{G}_{ijkl} \gamma_r \gamma_p * d\alpha_s * d\alpha_q d\mathbf{V} \right] \underline{\varepsilon}_{klrs} \\
 & \qquad - \sum_{(r,s) \in Q_h} \left[ \int_{\mathbf{V}} \gamma_p \gamma_r \alpha_s * d\alpha_q d\mathbf{V} \right] \underline{\sigma}_{ijrs} = 0 \\
 & 3. \sum_{(p,q) \in Q_h} \left[ - \int_{\mathbf{V}} \gamma_{p,j} \gamma_r \alpha_s * d\alpha_q d\mathbf{V} + \int_{\mathbf{S}_D} n_j \gamma_r \gamma_p \alpha_s * d\alpha_q d\mathbf{S} \right] \underline{u}_{ipq} \\
 & \qquad + \sum_{(p,q) \in Q_h} \left[ \int_{\mathbf{V}} \gamma_p \gamma_r \alpha_s * d\alpha_q d\mathbf{V} \right] \underline{\varepsilon}_{ijpq} \\
 & \qquad = \sum_{(p,q) \in Q_h} \int_{\mathbf{S}_D} n_j \underline{\varphi}_{ipq} \gamma_r \gamma_p \alpha_s * d\alpha_q d\mathbf{S}
 \end{aligned}
 \tag{2.15}$$

It is possible to observe that the above system of equations possess the following form:

$$\begin{aligned}
 & K^{(1,1)} \underline{u} + K^{(1,2)} \underline{\varepsilon} + K^{(1,3)} \underline{\sigma} = f^{(1)}, \\
 & K^{(2,1)} \underline{u} + K^{(2,2)} \underline{\varepsilon} + K^{(2,3)} \underline{\sigma} = f^{(2)}, \\
 & K^{(3,1)} \underline{u} + K^{(3,2)} \underline{\varepsilon} + K^{(3,3)} \underline{\sigma} = f^{(3)},
 \end{aligned}
 \tag{2.16}$$

where matrix  $\mathbf{K} = \begin{bmatrix} K^{(1,1)} & K^{(1,2)} & K^{(1,3)} \\ K^{(2,1)} & K^{(2,2)} & K^{(2,3)} \\ K^{(3,1)} & K^{(3,2)} & K^{(3,3)} \end{bmatrix}$  complies with the stiffness matrix of the structure determined by submatrices  $K^{(i,j)}$ ,  $(i, j = 1, 2, 3)$ ;  $(K^{(i,j)} = -K^{(j,i)^T})$ .

Vectors (in general tensors):

$$\underline{u} = \left\{ \underline{u}_{ipq} \right\}_{(p,q) \in Q_h}^{i=1,2,3}, \quad \underline{\varepsilon} = \left\{ \underline{\varepsilon}_{ijpq} \right\}_{(p,q) \in Q_h}^{i,j=1,2,3}, \quad \underline{\sigma} = \left\{ \underline{\sigma}_{ijpq} \right\}_{(p,q) \in Q_h}^{i,j=1,2,3}.$$

are the sought approximate solutions of the corresponding fields of displacements, strains and stresses.

From the system of Eqs. (2.15) it is possible to deduce formulae for the components of submatrices  $K^{(i,j)}$  and also components of generalized forces vector, i.e.:

$$\begin{aligned} K^{(1,1)} &= [0], & K^{(1,2)} &= [0], \\ K^{(1,3)} &= \left[ \int_{\mathbf{V}} \gamma_{p,j} \gamma_r \alpha_s * d\alpha_q d\mathbf{V} - \int_{S_D} n_j \gamma_p \gamma_r \alpha_s * d\alpha_q d\mathbf{S} \right], \\ (2.17) \quad K^{(2,1)} &= [0], & K^{(2,2)} &= \left[ \int_{\mathbf{V}} \tilde{G}_{ijkl} \gamma_r \gamma_p * d\alpha_s * d\alpha_q d\mathbf{V} \right], \\ & & K^{(2,3)} &= \left[ \int_{\mathbf{V}} \gamma_p \gamma_r \alpha_s * d\alpha_q d\mathbf{V} \right], \\ K^{(3,1)} &= \left[ - \int_{\mathbf{V}} \gamma_{p,j} \gamma_r \alpha_s * d\alpha_q d\mathbf{V} + \int_{S_D} n_j \gamma_r \gamma_p \alpha_s * d\alpha_q d\mathbf{S} \right], \\ & & K^{(3,2)} &= \left[ \int_{\mathbf{V}} \gamma_p \gamma_r \alpha_s * d\alpha_q d\mathbf{V} \right], & K^{(3,3)} &= [0], \\ (2.18) \quad f^{(1)} &= \sum_{(r,s) \in Q_h} \left[ \int_{\mathbf{V}} \underline{f}_{irs} \gamma_p \gamma_r \alpha_s * d\alpha_q d\mathbf{V} + \int_{S_F} \underline{\psi}_{irs} \gamma_p \gamma_r \alpha_s * d\alpha_q d\mathbf{S} \right], \\ f^{(2)} &= 0, \\ f^{(3)} &= \sum_{(p,q) \in Q_h S_D} \int \underline{\varphi}_{ipq} \gamma_r \gamma_p n_j \alpha_s * d\alpha_q d\mathbf{S}. \end{aligned}$$

Let us consider, finally, a case of variational formulation, which is most frequently encountered in FEM analysis, i.e. the formulation in the conditions of only one field, namely, the displacement field  $u$ . The functional of potential energy that corresponds to the formulation has a much simpler form:

$$(2.19) \quad J(u) = \frac{1}{2} \int_{\mathbf{V}} G_{ijkl} * d\varepsilon_{kl} * d\varepsilon_{ij} d\mathbf{V} - \int_{\mathbf{V}} f_i * du_i d\mathbf{V} - \int_{S_F} \sigma_{ij} n_j * du_i d\mathbf{S}.$$

Performing discretisation similarly to the Washizu-Reissner case, one formulates the approximating functions  $\gamma_p(x)$  and  $\alpha_q(t)$ . Thus, the corresponding approximate values of the vector fields may be expressed in the following way:

$$\begin{aligned}
 u_i(x, t) &= \sum_{(p,q) \in Q_h} \underline{u}_{ipq} \gamma_p(x) \alpha_q(t), \\
 \varepsilon_{ij}(x, t) &= \sum_{(p,q) \in Q_h} \underline{\varepsilon}_{ijpq} \gamma_p(x) \alpha_q(t) = \sum_{(p,q) \in Q_h} \underline{u}_{ipq} \gamma_{p,j}(x) \alpha_q(t), \\
 (2.20) \quad \sigma_{ij}(x, t) &= \sum_{(p,q) \in Q_h} \underline{\sigma}_{ijpq} \gamma_p(x) \alpha_q(t), \\
 f_i(x, t) &= \sum_{(p,q) \in Q_h} \underline{f}_{ipq} \gamma_p(x) \alpha_q(t), \\
 p_i(x, t) &= \sum_{(p,q) \in Q_h} \underline{p}_{ipq} \gamma_p(x) \alpha_q(t),
 \end{aligned}$$

After inserting Eq. (2.20) into Eq. (2.19) we obtain the following form of the approximation functional:

$$\begin{aligned}
 (2.21) \quad J(u_h) &= \sum_{(p,q) \in Q_h} \sum_{(r,s) \in Q_h} \left[ \frac{1}{2} \int_{\mathbf{V}} G_{ijkl} \underline{u}_{kr} \underline{u}_{ipq} \gamma_r^l \gamma_{p,j} * d\alpha_s * d\alpha_q d\mathbf{V} \right. \\
 &\quad \left. - \int_{\mathbf{V}} \underline{f}_{irs} \underline{u}_{ijq} \gamma_p \gamma_r \alpha_s * d\alpha_q d\mathbf{V} \right] - \int_{\mathbf{S}_F} \underline{p}_{irs} \underline{u}_{ipq} \gamma_p \gamma_r \alpha_s * d\alpha_q d\mathbf{S}.
 \end{aligned}$$

From the stationary condition  $\delta J(u_h) = 0$  we have the system of equations of the form:

$$(2.22) \quad \mathbf{K} \underline{u} = \underline{F},$$

i.e.:

$$\begin{aligned}
 &\sum_{(r,s) \in Q_h} \left[ \int_{\mathbf{V}} G_{ijkl} \gamma_r^l \gamma_{p,j} * d\alpha_s * d\alpha_q d\mathbf{V} \right] \underline{u}_{kr} \\
 &= \sum_{(r,s) \in Q_h} \left[ \int_{\mathbf{V}} \underline{f}_{irs} \gamma_p \gamma_r \alpha_s * d\alpha_q d\mathbf{V} + \int_{\mathbf{S}_F} \underline{p}_{irs} \gamma_p \gamma_r \alpha_s * d\alpha_q d\mathbf{S} \right]
 \end{aligned}$$

where the stiffness matrix and the force vector are expressed as follows:

$$(2.23) \quad \mathbf{K} = \left[ \int_{\mathbf{V}} G_{ijkl} \gamma_r, l \gamma_{p,j} * d\alpha_s * d\alpha_q d\mathbf{V} \right],$$

$$(2.24) \quad \underline{F} = \sum_{(r,s) \in Q_h} \left[ \int_{\mathbf{V}} \underline{f}_{irs} \gamma_p \gamma_r \alpha_s * d\alpha_q d\mathbf{V} + \int_{\mathbf{S}_F} \underline{p}_{irs} \gamma_p \gamma_r \alpha_s * d\alpha_q d\mathbf{S} \right].$$

Equation (2.22) is the fundamental expression used in the numerical FEM package that is used during the realisation of the numerical calculation, where the generalized material tensor  $G$  describing the time-variable viscoelastic properties takes the particular form as shown by (2.1).

### 3. RESULTS

The above model was subjected to computer-aided strength analysis using the ANSYS system. Changes with time of the Huber – von Misses stresses ( $\sigma^{eqv}$ ), strains ( $\varepsilon^{eqv}$ ) and strain energy density ( $A$ ) were observed. The dimensionless coefficients were employed in the description:

$$(3.1) \quad {}^t_t \varepsilon^{eqv} = \varepsilon_t^{eqv} / \varepsilon_{t_0}^{eqv}, \quad {}^t_t \sigma^{eqv} = \sigma_t^{eqv} / \sigma_{t_0}^{eqv}, \quad {}^t_t A = A_t / A_{t_0}$$

which represent the relation on of the value of a given parameter at time  $t$  to its value at time  $t_0$ . Strain energy density in ANSYS system is calculated from the following relationship:

$$(3.2) \quad A = \frac{1}{vol_{el}} \left( \frac{1}{2} \sum_{i=1}^{NINT} \{\sigma\}^T \{\varepsilon^{el}\} vol_i + E^{pl} \right)$$

where: NINT – number of Gauss points in volume of a given finite element,  $vol_i$  – volume surrounding  $i$ -th Gauss point,  $vol_{el}$  – volume of element,  $\{\sigma\}$  – stress vector,  $\{\varepsilon^{el}\}$  – elastic strain vector,  $E^{pl}$  – plastic strain energy.

In such a system subjected to a fixed load, as time passes, a process of bone creep occurs in both the cortical and trabecular bone, though with different intensities in each of them. Trabecular bone creep occurs quickly and practically stabilises after several minutes, whereas significant strain changes can be observed in cortical bone for a much longer time of the order of several dozens of minutes or even several hours. The distribution of dimensionless coefficients (as in Eq. (3.1)) for time  $t_1 = 160$  sec is shown in Fig. 5 (the implant made of titanium alloy,

support of the endoprosthesis through an intermediate layer of trabecular bone – model M1).

During this period, trabecular bone creep dominates (Fig. 5a). The increase of strain, however, in the major part of the volume of tissue, does not reach the value resulting from the applied model, due to internal redistribution of stresses in the implant – trabecular bone – cortical bone system (Fig. 5b).

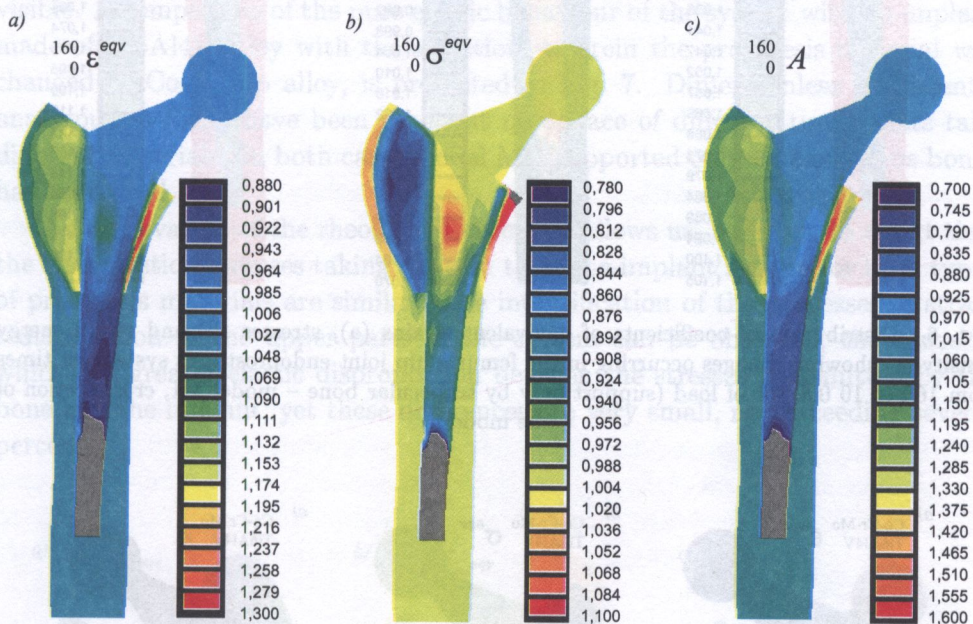


FIG. 5. Distribution of coefficients of equivalent strains (a), stresses (b) and strain energy density (c) showing changes occurring in the femur - hip joint endoprosthesis system for the first 160 sec of load (support only by trabecular bone – model M1, cross-section of the model).

The changes observed over longer periods of time occur much more slowly than in the first two minutes. A comparison of strains, stresses, and strain energy density at time  $t_2 = 10000$  sec (about 2 h 45') with the state at time  $t_1 = 160$  sec is shown in Fig. 6.

During this period, the cortical bone creep phenomenon plays a decisive role. Increase of strain in the area of cortical tissue reaches about 10%. The stress redistribution in the implant – trabecular bone – cortical bone structure is a result of the bone creep. However, this redistribution is of a different character. In the cortical bone region, there is a decrease of stresses, these being taken over by the interior layer of trabecular bone or implant.

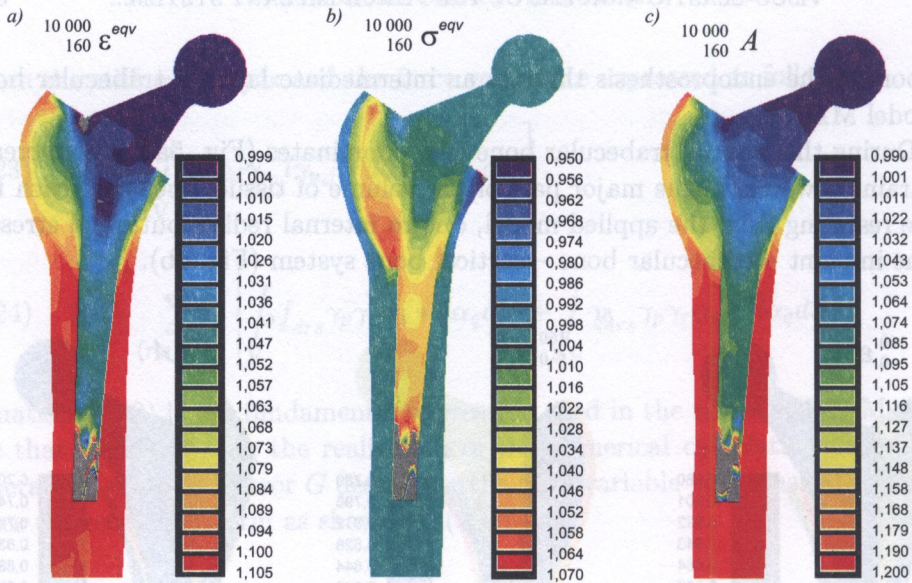


FIG. 6. Distribution of coefficients of equivalent strains (a), stresses (b) and strain energy density (c) showing changes occurring in the femur – hip joint endoprosthesis system for times from 160 to 10 000 sec of load (support only by trabecular bone – model M1, cross-section of the model).

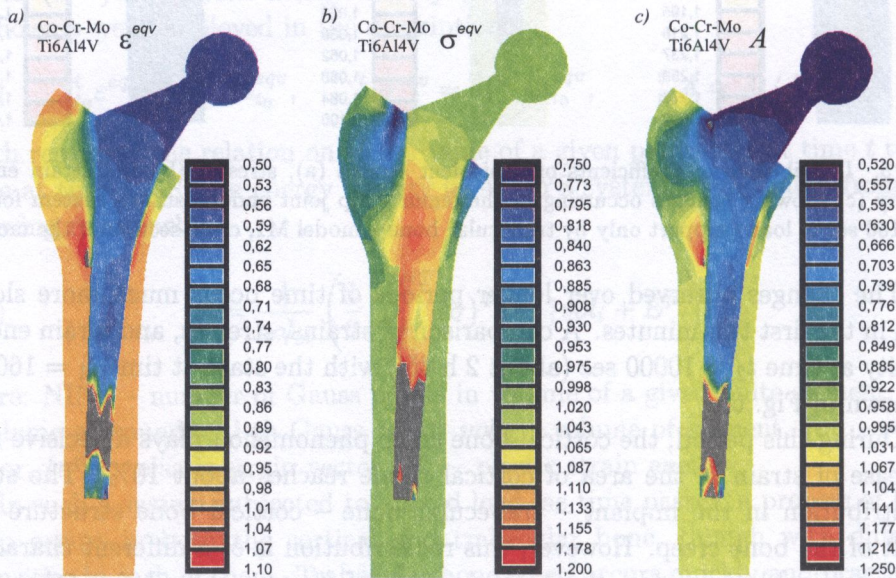


FIG. 7. Distribution of coefficients of equivalent elastic strains (a), stresses (b) and strain energy density (c) showing changes occurring between model with stem made of CoCrMo alloy and Ti6Al4V alloy (support only by trabecular bone – model M1, cross-section of the model).

In the case of the change of the endoprosthesis stiffness (the Co-Cr-Mo alloy in place of Ti6Al4V), significant changes in the distribution of elastic stresses and strains in the bone implant system are observed. The stress shielding effect is more evident. The decrease of strain in the upper regions of the femur reaches 20% in comparison with the system containing the titanium implant. Also, a concentration of strains in the distal end of the zone of implant-bone contact is visible. A comparison of the pure elastic behaviour of the system with an implant made of Ti6Al4V alloy with the situation, wherein the prosthesis material was changed to Co-Cr-Mo alloy, is presented in Fig. 7. Dimensionless coefficients, analogous to (3.1), have been used but now place of different time points take different materials. In both cases model M1 (supported only by cancellous bone) has been used.

An observation of the rheological processes allows us, however, to assert that the viscoelastic processes taking place in the bone-implant system for both types of prosthesis materials are similar. The intensification of the processes of strain redistribution in the upper parts of the system can be observed, the cause of which is a greater elastic disproportion between the stresses transmitted by the bone and the implant, yet these differences are very small, not exceeding several percent.

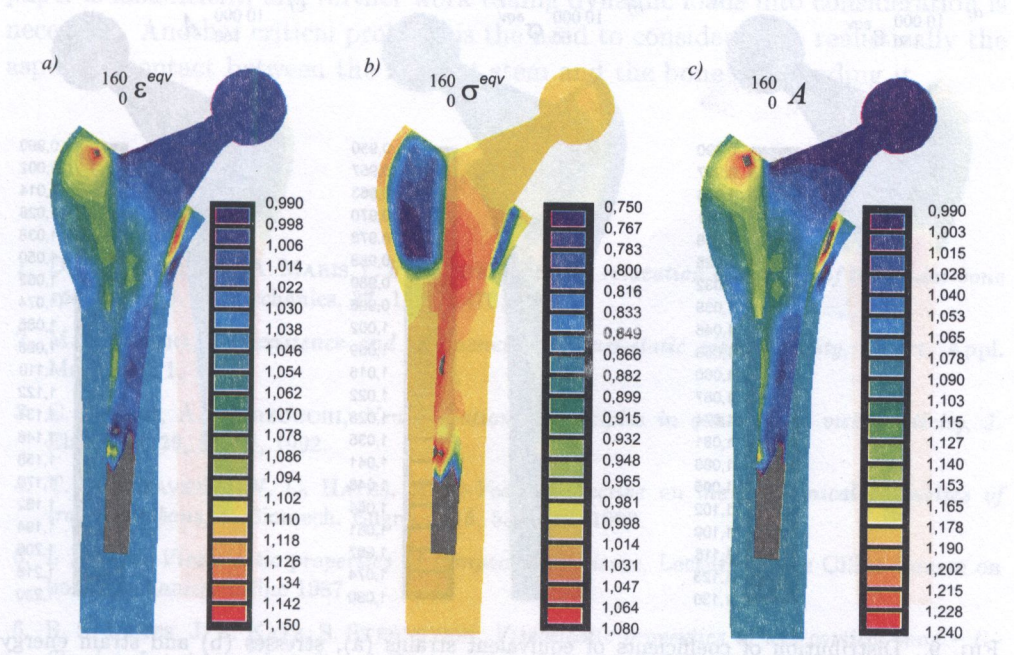


FIG. 8. Distribution of coefficients of equivalent strains (a), stresses (b) and strain energy density (c) showing changes occurring in the femur – hip joint endoprosthesis system for times from 0 to 160 sec of load in the model with partial support by cortical bone (model M2 – cross-section of the model).

The course of rheological processes is influenced to a much greater extent by the method of implant support. In the case of direct contact between the prosthesis stem and cortical bone, which may occur in practice, much lower elastic stresses and strains appear in the upper part of the femur than in the case of support through an intermediate layer of trabecular bone (the difference reaching even 60 – 70%). With time, a redistribution of stresses between trabecular and cortical bone takes place, and there is an increase in the significance of redistribution in the bone-implant system. This increase of stress in the upper part of the stem can reach 20%. If we consider that the initial proportions between the load transmitted by the bone and the implant are disadvantageous, the later increase in the role played by the stem must lead to a deepening of the stress shielding phenomenon, which in the long term may result in the atrophy of the bone tissue in the proximal region. Distribution of coefficients of effective strains (a), stresses (b) and strain energy density (c) in the bone-implant system for an implant partly supported by cortical bone (model M2) are given in Fig. 8 (short time of observation: 0 – 160 sec) as well as in Fig. 9 (long time of observation: 160 – 10000 sec).

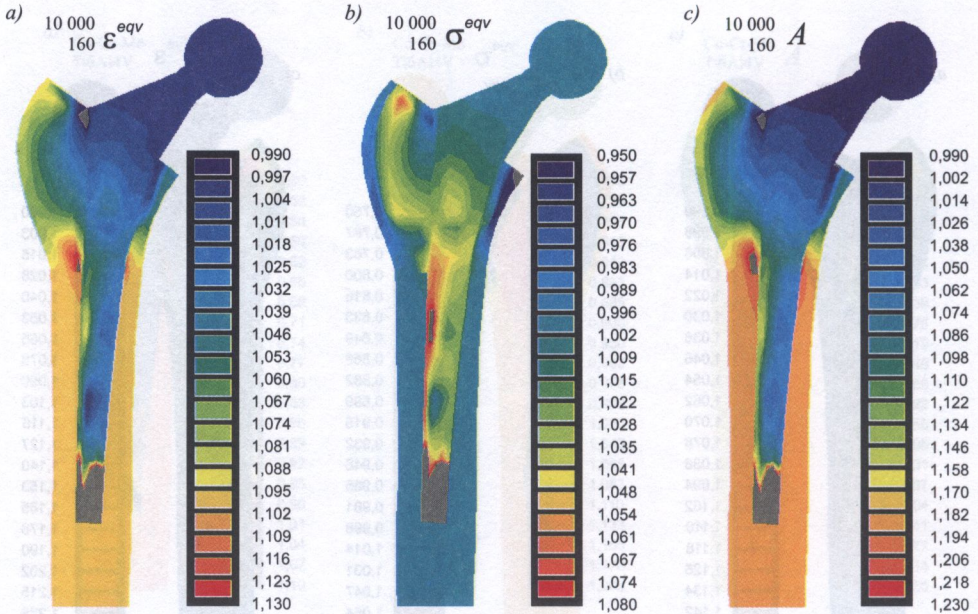


FIG. 9. Distribution of coefficients of equivalent strains (a), stresses (b) and strain energy density (c) showing changes occurring in the femur – hip joint endoprosthesis system for times from 160 to 10 000 sec of load in the model with partial support by cortical bone (model M2 – cross-section of the model).

#### 4. CONCLUSION

From the presented numerical results, it appears that the implant – femur system, subjected to strength analysis taking into account the viscoelastic properties of bone tissue, displays a series of differences from a system analysed exclusively in terms of elastic deformations. In the case of quasi-static loads, as analysed in this paper, the observed changes are related primarily to bone tissue creep, which results in the redistribution of stresses within the system. Especially in the proximal part of the system, the implant takes over the major part of the load, and this is an undesirable phenomenon. It increases the so-called stress shielding effect, resulting in the atrophy of bone tissue in regions of excessive unload. Consideration of the viscoelasticity of bone tissue makes it possible not only to estimate quantitatively the changes of stress and strain occurring during the time of load, but also to analyse how the heterogeneous bone structure reacts to the applied loads and to describe the character of the processes taking place in such conditions. This facilitates a more complete understanding of the functioning of the implanted joint, and opens the way towards the improvement of endoprosthesis construction.

It is necessary to emphasise that the quasi-static analysis presented in this paper is insufficient, and further work taking dynamic loads into consideration is necessary. Another critical problem is the need to consider more realistically the aspect of contact between the implant stem and the bone surrounding it.

#### REFERENCES

1. D. D. DELIGIANNI, A. MARIS, Y. F. MISSIRLIS, *Stress relaxation behaviour of trabecular bone specimens*, J. Biomechanics, **27**, 1469–1476, 1994.
2. M. FABRIZIO, *An existence and uniqueness in quasi-static viscoelasticity*, Quart. Appl. Math., **47**, 1, 1987.
3. C. GIORGI, A. MARZOCCHI, *New variational principles in quasi-static viscoelasticity*, J. Elasticity, **29**, 86–96, 1992.
4. T. M. KEAVENY, W. C. HAYES, *A 20-Year perspective on the mechanical properties of trabecular bone*, J. Biomech. Engng., **115**, 534–542, 1993.
5. I. KNETS, *Viscoelastic properties of compact bone tissue*, Lecture at the CISM Course on bone mechanics, Udine 1987.
6. R. S. LAKES, J. L. KATZ, S. STERNSTEIN, *Viscoelastic properties of wet cortical bone – I – Torsional and biaxial studies*, J. Biomechanics, **12**, 657–678, 1979.
7. A. N. NATALI, E. A. MEROI, *A review of the biomechanical properties of bone as a material*, J. Biomed. Engng., **11**, 266–276, 1989.

8. S. PISZCZATOWSKI, K. SKALSKI, G. SLUGOCKI, A. WAKULICZ, *Finite element method formulation for the interactions between various elastic-viscoelastic structures in biomechanical model*, [In:] Computer Methods in Biomechanics & Biomedical Engineering – 2, J. MIDDLETON, M. L. JONES, G. N. PANDE [Eds.], Gordon and Breach Science Publishers, 1998 Amsterdam.
9. B. RIETBERGEN, R. HUISKES, H. WEINANS, D. R. SUMNER, T. M. TURNER, J. O. GALANTE, *The mechanism of bone remodeling and resorption around press-fitted THA stems*, J. Biomechanics, **26**, 369–382, 1993.
10. N. SASAKI, A. ENYO, *Viscoelastic properties of bone as a function of water content*, J. Biomechanics, **28**, 809–815, 1995.
11. M. VICECONTI, M. CASALI, B. MASSARI, L. CRISTOFOLINI, S. BASSINI, A. TONI, *The “Standardised Femur Program” proposal for a reference geometry to be used for the creation of finite element models of the femur*, J. Biomechanics, **29**, 1241, 1996.
12. K. WASHIZU, *Variational methods in elasticity and plasticity*, Pergamon Press, New York 1968.

Received February 2, 2001.

---